Molecular and Electronic Structure of Zinc Carbyne, HZnCH, and Zinc Stannyne, HZnSnH, from ab Initio Calculations

ARTICLE *in* THE JOURNAL OF PHYSICAL CHEMISTRY · JANUARY 1996

Impact Factor: 2.78 · DOI: 10.1021/jp952199l

3 AUTHORS, INCLUDING:

Miguel San-Miguel
University of Campinas
53 PUBLICATIONS **749** CITATIONS
SEE PROFILE

Antonio M Márquez
Universidad de Sevilla
84 PUBLICATIONS **1,348** CITATIONS
SEE PROFILE

Molecular and Electronic Structure of Zinc Carbyne, HZnCH, and Zinc Stannyne, HZnSnH, from *ab Initio* Calculations

M. A. San Miguel, A. Márquez, and Javier Fernández Sanz*

Departamento de Química Física, Facultad de Química, E-41012, Seville, Spain

Received: August 2, 1995; In Final Form: October 17, 1995[⊗]

The electronic and molecular structures of both the ground state and some excited states of zinc carbyne and zinc stannyne have been investigated using ab initio Hartree−Fock second order Moller−Plesset (MP2) and complete active space self-consistent-field (CASSCF) calculations. The ground state of HZnCH is the triplet $^3\Sigma^-$ in agreement with experiment and previous theoretical work, while the first excited state, the $^1\Delta$ state, shows a classical distortion of the Renner−Teller type. The bond mechanism in these compounds has been carefully analyzed, and particularly the possibility of the presence of a Zn−C double bond is discussed. In contrast with zinc carbyne, the ground state of zinc stannyne is a singlet $^1A'$ while the first excited state is a triplet $^3A''$. These states can be viewed as arising from nonclassical distortions featured by the corresponding $^3\Sigma^-$ and $^1\Delta$ states due to strong electronic coupling. This loss of linearity has been related to the split between s−p tin levels and with the models proposed for nonclassical distortions at multiple bonds.

1. Introduction

In the last few years the chemistry of transition organometallic compounds has deserved considerable effort, mainly due to their use in homogeneous and heterogeneous catalysis.[4] Understanding the metal−carbon bond nature in these compounds plays a key role in the interpretation of both their properties and their reactivity, and nowadays the metal−carbon bond in methyl and methylene (carbene) derivatives is a well-established notion.[5−7] Properties of transition metal methylidynes are less known, principally because of the lack of small unligated samples suitable for realistic theoretical analysis. The first unligated hydride zinc methylidyne was isolated and spectroscopically characterized by Chang *et al.* in 1987.[1] This prototypical zinc carbyne was obtained from photolysis of zinc carbene $ZnCH_2$ trapped in an argon matrix, and, on the basis of FTIR data, the presence of a triple Zn≡C bond was suggested. Effectively, there is a shift of the Zn−C IR frequency from 447 cm^{-1} in $HZnCH_3$ to 513 cm^{-1} in $ZnCH_2$ and to 647 cm^{-1} in HZnCH, suggesting that a significant π bond takes place. Hamilton and Shaefer reported later[2] on a theoretical study about the molecular structure of $ZnCH_2$ and HZnCH and concluded that the Zn−C bond should be single in the carbene and double in the carbyne.

In a recent paper[8] we have reported a theoretical analysis on the electronic structure of some zinc carbene based complexes as well as on the zinc carbene−zinc carbyne photorearrangement. In that work the possibility of nonclassical distortions was also considered and we were able to show that the ground state of $ZnSnH_2$ (a singlet) was largely distorted. Such a type of structure was also found in a closely related molybdenum derivative, $MoSnH_2$, showing that, as predicted by Trinquier and Malrieu,[3] nonclassical distortions at multiple bonds leading to nonplanar geometries would also happen in transition metal derivatives.[9] In the models derived by these authors, nonclassical distortions at the multiple bond did not concern only deviations from planarity but also deviations from linearity, and, for instance, silaacetylene (or silaethyne) HSi≡CH was predicted to be trans bent instead of linear as its parent acetylene, HC≡CH. However, as far as we can ascertain, extensions of this model to linear transition metal complexes have not been reported.

In the present paper we report a theoretical study based on ab initio quantum mechanical calculations of the zinc carbyne and zinc stannyne electronic and molecular structure. The first goal of this work is to analyze the nature of the zinc−carbon bond in zinc carbyne, and with this aim, the geometry of this compound has been determined at various levels of theory and a full vibrational analysis has been performed. Second, in order to analyze the possibility of nonclassical distortions in these types of compounds, a parallel analysis of zinc stannyne has also been carried out in this direction.

2. Computational Details

Ab initio calculations were undertaken using the effective core potential (ECP) reported by Stevens *et al.*[10] to describe inner electrons of zinc and tin atoms. For valence electrons of zinc (3s, 3p, 3d, and 4s) the basis set was (8s8p6d) contracted to [4s4p3d]. For the tin atom, only the 5s 5p electrons were explicitly taken into account using a (5s5p1d)/[2s2p1d] basis set. For C and H atoms the standard DZP basis set was used.[11] Open shells were handled through both unrestricted Hartree−Fock (UHF) and complete active space SCF (CASSCF) wave functions.[12] In the UHF calculations, dynamical electron correlation was incorporated through second order perturbational theory under the Moller−Plesset partition (UMP2). The molecular orbitals (MOs) in the active space of the CASSCF wave functions were σ_{XH}, σ_{HZn}, σ_{ZnX}, and their σ antibonding partners as well as the open shell pair $\pi_{x,y}$ holding the two lone electrons (i.e., 8 electrons/8 MOs).

Molecular geometries were optimized using standard analytical gradient techniques, and stationary points were then characterized by computation and further diagonalization of the matrix of second derivatives of the energy $\mathbf{F}^x$ in a Cartesian coordinate representation. In order to obtain a set of physically meaningful force constants in terms of internal symmetry coordinates,[9] the $\mathbf{F}^x$ matrix was then transformed using the **B** matrix. All the calculations were performed using GAUSSIAN-92[13] (unrestricted MP2 calculations) and HONDO-8[14] (CASSCF calculations) programs running on a Convex C-240.

3. Results and Discussion

3.1. Structure of Zinc Carbyne (HZnCH). The structural parameters optimized at several levels of theory for both HZnCH

[⊗] Abstract published in *Advance ACS Abstracts,* December 15, 1995.

0022-3654/96/20100-1600$12.00/0

TABLE 1: Optimized Bond Distances (Å) and Bond Angles (deg) for HZnCH

	HF	MP2	CASSCF	CISD[a]
$^3\Sigma^-$				
d(Zn−C)	1.9163	1.8633	1.9405	1.883
d(C−H)	1.0761	1.0794	1.0960	1.083
d(Zn−H)	1.5474	1.5010	1.5743	1.521
$^1A'$				
d(Zn−C)	1.9973	1.9392	2.0651	
d(C−H)	1.0933	1.1027	1.1290	
d(Zn−H)	1.5585	1.5142	1.5922	
∠HCZn	117	117	109	
∠HZnC	174	172	173	

[a] Reference 2.

and HZnSnH are summarized in Tables 1 and 2. Whatever the level of calculation is, the ground state of HZnCH is found to be a triplet of linear geometry, state $^3\Sigma^-$, in contrast to the results of Hamilton *et al.*[2] who reported a bent structure at the Hartree−Fock level and linear when electron correlation was incorporated. This narrow dependence of the structure on the wave function type has already been found in other organometallic compounds and interpreted in terms of nondynamical correlation effects.[15] When the different values are compared, the well-known evolution of the bond distances is found. Thus, on going from the UHF to UMP2 values, there is a lengthening of the strong bonds (the CH), and a shortening of the weak bonds (Zn−C and Zn−H). With respect to CASSCF results, a general lengthening of the bond distances is observed because of the inclusion of the σ antibonding MOs in the active space.

The electronic structure of HZnCH can be rationalized in terms of its fragments HZn and CH. The ground state of HZn is a $^2\Sigma^+$ state (σ_{sp}^1 configuration), while that of CH is a $^2\Pi$ one ($\sigma^2\ \pi^1$ configuration). Interaction of these states leads to a singlet $^1\Pi$ and a triplet $^3\Pi$, and, therefore, dissociation of the carbyne ground state does not correlate directly with the ground state of its constitutive fragments. However, the correlation is direct toward the first excited state of CH, the quartet $^4\Sigma^-$ ($\sigma^1\ \pi_{xy}^2$ configuration), as shown in Figure 1, where dissociation curves for zinc carbyne obtained from CASSCF calculations are reported. As can be seen in this figure, there is an allowed crossing between the $^3\Sigma^-$ state and the $^1\Pi$ and $^3\Pi$ states which are those leading to the ground state of fragments. After these preliminary considerations, the Zn−C bond can be easily understood from the MO diagram of Figure 2. The $^4\Sigma^-$ state has a lone electron in a C σ_{sp} orbital (the 3σ MO), which pairs with the Zn σ_{sp} electron, while the two C π_{xy} electrons remain in a π MO leading for a triplet arrangement to a $^3\Sigma^-$ state:

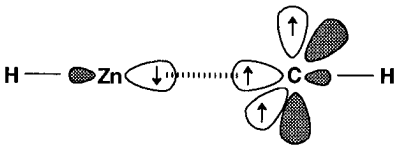

The analysis of these π MO shows that they correspond mainly to the C $p_{x,y}$ atomic orbitals, suggesting that the Zn−C bond is essentially single, without significant π donation from the C

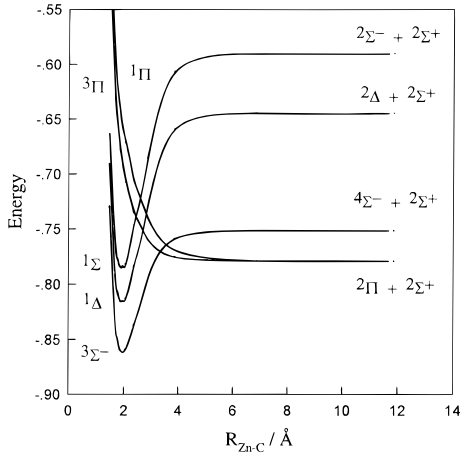

Figure 1. Potential energy profiles for dissociation of HZnCH from CASSCF calculations. The asymptotic labels refer to the final states of CH and HZn fragments. In these curves the CH and HZn interatomic bond distances are fixed.

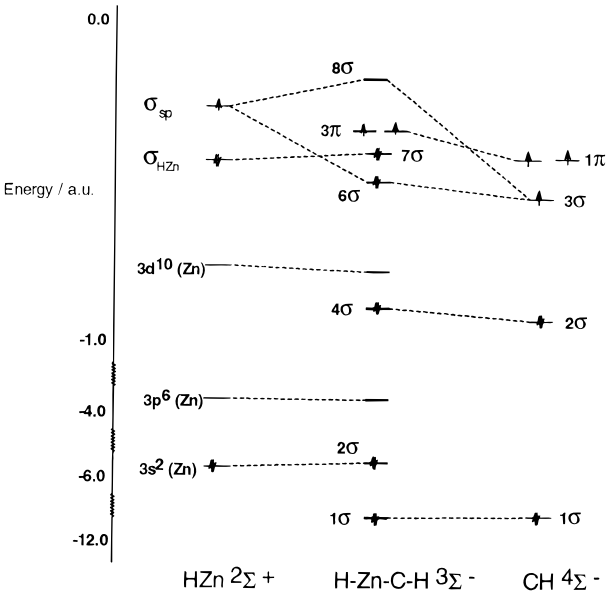

Figure 2. Molecular orbital diagram for the $^3\Sigma^-$ state of HZnCH.

$p_{x,y}$ occupied MO toward the Zn $p_{x,y}$ empty pair. The lack of π bond is consistent with the higher electronegativity of carbon and agrees with a net spin population of 1.98 computed for carbon, as well as with the Zn−C bond order[16] (0.89), close to that estimated for $ZnCH_2$ (0.84 for the triplet $^3B_1$ at the UHF level).

On the other hand, as also shown in Figure 1, the first excited state of HZnCH is a singlet $^1\Delta$ arising from the interaction of the HZn ground state and the $^1\Delta$ state of CH. As is well-known, vibronic coupling in electronic degenerate states of linear polyatomic molecules provides a mechanism for distortions and, therefore, for the loss of linearity (Renner−Teller effect).[17] In the absence of strong electronic coupling with other states, Δ electronic states are predicted[18] to be minima on the potential energy hypersurface (PES), and if the coupling with the bending

TABLE 2: Optimized Bond Distances (Å) and Bond Angles (deg) for HZnSnH

	$^3\Sigma^-$ state			$^3A''$ state			$^1A'$ state		
	HF	MP2	CASSCF	HF	MP2	CASSCF	HF	MP2	CASSCF
d(Zn−Sn)	2.5916	2.5385	2.5437	2.5916	2.5385	2.6050	2.7409	2.6727	2.7867
d(Sn−H)	1.7083	1.7092	1.7160	1.7083	1.7092	1.7484	1.7648	1.7676	1.8028
d(Zn−H)	1.5666	1.5232	1.5822	1.5666	1.5232	1.5948	1.5906	1.5446	1.6213
∠HZnSn				176	176	177	178	178	178
∠HSnZn				126	125	126	91	90	91

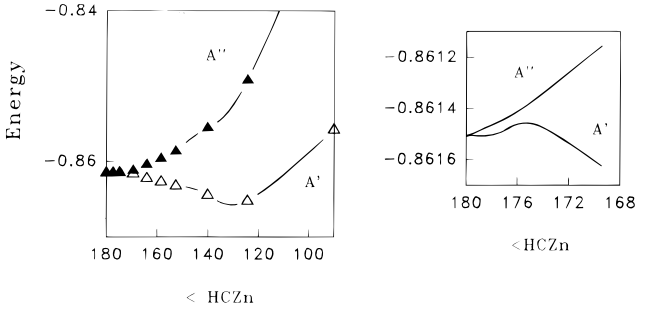

Figure 3. Potential energy profiles obtained from CASSCF calculations showing the classical Renner−Teller effect featured by the Δ states of HZnCH. The zoom for small HCZn bending angles (on the right) shows how these states are in fact true mimima on the surface.

coordinate is large enough, a second minimum on the PES is observed for larger values of the bending coordinate. This is precisely the behavior observed in the $^1\Delta$ state of HZnCH as shown in Figure 3, where the cross section potential energy is plotted against the HCZn bond angle. As can be seen, $^1\Delta$ states split into A′ and A″ states, both of them having higher energies for small values of the bending angle; however, after a low barrier, a stabilization of the A′ component is observed leading to a minimum for an HCZn angle close to 120°. Optimization (Table 1) and Hessian calculation of this C_s structure show it to be a true minimum on the PES, the energy difference between the $^3\Sigma^-$ and the ^{1}A′ states being 51.8 kcal/mol at the MP2 level. The bond between zinc and carbon in this compound can be depicted as a σ bond formed by a pairing of the HZn sp_σ electron with a carbon sp_σ one, the carbon remaining in a sp^2 like hybridization:

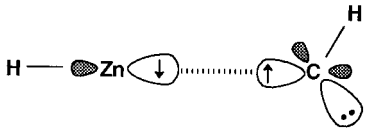

3.2. Structure of Zinc Stannyne (HZnSnH). We now consider the electronic structure of zinc stannyne (HZnSnH). Under $C_{\infty v}$ symmetry constraint, the lowest electronic state is also a $^3\Sigma^-$ whose electronic configuration is similar to that of zinc carbyne. However, whatever the calculation level is, this structure is not a true minimum on the potential energy surface and its vibrational analysis shows two imaginary frequencies (405 cm^{-1}, CASSCF) associated to a degenerate normal mode of a trans-bending type. In fact, the linear structure corresponds to a saddle point interconnecting the two equivalent isomers of C_s symmetry, states ^{3}A″, in which a loss of linearity is observed. The barrier for the interconversion of the two C_s structures is 6.3 kcal/mol at the CASSCF level:

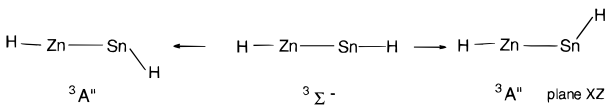

The electronic structure of these ^{3}A″ states can be easily understood starting from the model for the $^3\Sigma^-$ of carbyne reported above. As for HZnCH, the $^3\Sigma^-$ state arises from interaction between the $^4\Sigma^-$ of SnH and the $^2\Sigma^+$ states of HZn. After pairing the σ_{sp} electrons, there are two electrons left in a π_{xy} MO; however, the weak (if any) π bond between Sn and Zn does not compensate for the higher energetic gap between the s and p levels of tin, and therefore the mix of s and p tin orbitals allowed through distortion stabilizes the system. In

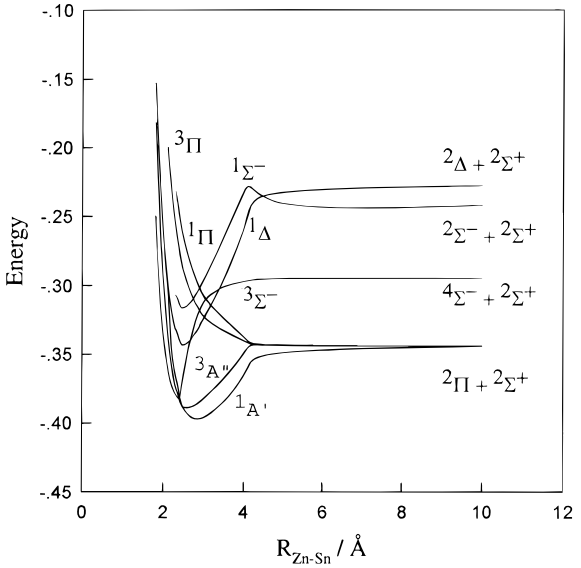

Figure 4. Potential energy profiles for dissociation of HZnSnH from CASSCF calculations. The asymptotic labels refer to the final states of SnH and HZn fragments. These curves are only qualitative since HZn and SnH interatomic bond distances have been kept fixed. In ^{1}A′ and ^{3}A″ states the HSnZn angle is also fixed to their equilibrium values.

other words, this sp hybridization gives place to a stabilization of one π_{xy} electron, the other remaining in a perpendicular MO (a″):

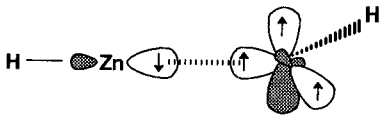

Notice that this interpretation is based on the relative s−p gaps of carbon and tin, but it is essentially equivalent to that proposed by Trinquier and Malrieu,[3] since these authors rationalize the loss of linearity in terms of energy differences between the ground state and the quartet state ($^2\Pi-^4\Sigma^-$ split). We have not looked for an accurate calculation of this split in SnH, but even at the CASSCF level the $^2\Pi-^4\Sigma^-$ split for SnH is found to be about 38 kcal/mol, i.e., roughly twice the split proposed for CH (17 kcal/mol [19]).

On the other hand, as for carbyne, the first excited state of HZnSnH under the $C_{\infty v}$ constraint is the singlet $^1\Delta$ (see Figure 4). This state is also expected to distort by vibronic coupling; however, the electronic coupling is now very strong, and the usual shape of the Renner−Teller effect for these types of states is no longer observed. Instead, the ^{1}A′ component is largely stabilized upon distortion, leading to a C_s structure (Table 2), which is, in fact, the ground state of HZnSnH, the energy difference between the ^{1}A′ and ^{3}A″ being 24 kcal/mol. The electronic structure of this state can be depicted as arising from the $^2\Sigma^+$ state of HZn and the $^2\Pi$ state of SnH in a perpendicular interaction which is again governed by the already mentioned trend of tin electrons to remain in an s orbital:

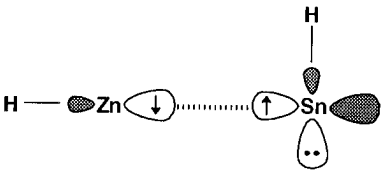

3.3. Vibrational Analysis of Zinc Carbene and Zinc Carbyne. The harmonic force constants of $ZnCH_2$ and HZnCH estimated from MP2 calculations as well as those deduced by

TABLE 3: Selected Force Constants for $ZnCH_2$ and HZnCH Ground States[a]

	MP2	fitted[b]	description
$ZnCH_2$			
f(ZnC)	2.045	2.348	Zn−C stretch
$f(CH)_s$	5.804	4.712	C−H sym stretch
$f(CH_2)_b$	0.476	0.410	CH_2 bend
$f(CH_2)_w$	0.193	0.174	CH_2 wag
$f(CH)_a$	5.853		C−H antisym stretch
$f(CH_2)_r$	0.134	0.088	CH_2 rock
HZnCH			
f(ZnC)	2.855	2.932	Zn−C stretch
f(CH)	6.144		C−H stretch
f(ZnH)	2.413	2.125	Zn−H stretch

[a] Stretching and bending force constants are in mdyn/Å and mdyn·Å, respectively. [b] Reference 1.

Chang *et al.* from the experimental spectra (anharmonic) are reported in Table 3. As can be seen, the ab initio values are higher than the "experimental" ones, in agreement with the harmonic nature of the former. The exceptions are the Zn−C force constants which are found to be somewhat lower, mainly for $ZnCH_2$ (0.3 mdyn/Å). As we have seen, the inclusion of electron correlation effects reinforces these bonds, and, therefore, it is expected that higher level calculations (and larger basis sets) will increase these metal−carbon force constants.

Using these moderately accurate force fields, harmonic frequencies for $ZnCH_2$ and HZnCH, as well as for their isotopic derivatives, have been determined (Tables 4 and 5). Inspection of these tables shows that (i) the theoretical values are in quite good agreement with both the experiment and the results of Hamilton *et al.*[2] and (ii) they are always larger than the experimental (anharmonic) frequencies according to the well-known trend,[20] the deviations falling in the 4−8% range with the exception of the wagging frequency which appears to be significantly overestimated (17% higher). This frequency appeared also to be overestimated in the work of Hamilton *et al.*[2] (restricted open shell Hartree−Fock force field), who suggested that it should be decreased by higher levels of calculation; however, neither the MP2 force field nor the CASSCF calculation (which gives 637 cm^{-1}) improves the result. In principle, the wagging frequency can be related with the extension of the π interaction between the carbon and the metal in the sense that the larger is the interaction, the higher has to be the wagging force constant since this vibration involves loss of the π overlap. This relationship is nicely observed in the MCH_2 series with M = Cr, Fe, Co, and Ni, where the increment of the stretching metal−carbon frequencies correlates with that of the CH_2 wag:[21] ν(M−C) = 567, 623, 655, and 696 cm^{-1}; $\nu(CH_2)_w$ = 688, 700, 757, and 791 cm^{-1}. Notice, on the other hand, that the $\nu(CH_2)_w$ are 80−100 cm^{-1} higher than the corresponding ν(M−C). However, while the metal−carbon frequency drops to 614 and 514 cm^{-1} for Cu and Zn carbenes, the CH_2 wag is dramatically lowered to 526 and 525 cm^{-1}, respectively. This analysis suggests that either there is an overestimation of the π interaction in the theoretical calculations or there is a cage effect in the argon solid matrix. Support for the theoretical result is given by the fact that for $MoCH_2$ the wagging frequency is computed[9] to be 716 cm^{-1}, in agreement with that of $CrCH_2$ (688 cm^{-1}).

Focusing now on the frequencies associated with the Zn−C bonds, it can be observed that the experimental shift observed on going from $ZnCH_2$ to HZnCH (114 cm^{-1}) is nicely reproduced by the MP2 calculations (118 cm^{-1}), showing the coherency of our force fields. Finally, as stated in the Introduction, this shift has been proposed as evidence of a π bond between Zn and C. However, as we have shown, the π MO is mainly localized on the carbon atom and there is not a significant bond order increment in HZnCH. As the larger force constant conclusively shows, there is a clear reinforcement in the Zn−C bond; however, it is not necessarily (or at least not totally) due to the existence of a π bond. There are other factors to be considered. First, the s character in the σ_{sp} MO is larger in CH than in CH_2 fragments. For instance, the CH vibrational frequency increases from 3250 cm^{-1} (mean value of symmetric and antisymmetric frequencies) in $ZnCH_2$ to 3358 cm^{-1} in HZnCH. Second, the Zn−C bond in $ZnCH_2$ corresponds formally to a two center, three electron interaction. In fact, this bond arises from the interaction of the ^{1}P Zn state and the $^3B_1$ state of CH_2. However, as we have shown in this work, the Zn−C bond in HZnCH corresponds to a strong interaction between two σ_{sp} orbitals leading to a well-behaved σ bond. Consequently, these two factors contribute to a higher strength of the bond without necessarily invoking the presence of a Zn−C π bond.

4. Summary and Conclusions

In this work we have carried out a theoretical study of the electronic structure of zinc carbyne and its homologous zinc stannyne. In agreement with experiment and previous calculations, the ground state of HZnCH is the triplet $^3\Sigma^-$. The bond in this complex arises from interaction between the first CH excited state (the quartet $^4\Sigma^-$) and the ground state of HZn (a doublet $^2\Sigma^+$). The open shell corresponds to a π^2 configuration built up mainly from the π_{xy} carbon orbitals, without significant contribution of Zn p_{xy} orbitals, suggesting therefore that a small π bond between Zn and C, if any, is present. This result seems to be in contradiction to the shift in the Zn−C IR frequency observed in the experimental spectra of $ZnCH_2$ and HZnCH as well as to the Zn−C force constants estimated for these complexes. However, we have argued that there are two effects more which allow for a stronger Zn−C interaction without invoking a π bond, namely, the increase of s character in the σ_{sp} orbital of CH with respect to CH_2 and the well-behaved nature of the HZn σ_{sp} MO.

The first excited state of HZnCH is a singlet $^1\Delta$. As predicted for linear degenerate states, this state features vibronic coupling, leading to a classical distortion of Renner−Teller type. A split of the Δ states gives place to a minimum of C_s symmetry ($^1A'$ state) in which the carbon is in a sp^2-like hybridization.

TABLE 4: Theoretical (ω/cm^{-1}) and Experimental[1] (ν/cm^{-1}) Vibrational Frequencies for $ZnCH_2$ and Isotopic Derivatives

	$ZnCH_2$			$Zn^{13}CH_2$		ZnCHD		$ZnCD_2$		
symmetry	ω	ω^a	ν	ω	ν	ω	ν	ω	ν	description
a_1	3198	3227	2956	3193	2953	2384	2220	2316	2166	C-H sym stretch
	1404	1475	1341	1398	1332	1245		1045	1010	CH_2 bend
	548	562	514	533	497	548	511	515	472	Zn-C stretch
b_1	638	621	525	632	516	573	470	499	419	CH_2 wag
b_2	3313	3315	3047	3300	3035	3260	3003	2461		C−H asym stretch
	570	569	544	567	541	468	445	430	412	CH_2 rock

[a] Hartree−Fock values from ref 2.

TABLE 5: Theoretical (ω/cm^{-1}) and Experimental[1] (ν/cm^{-1}) Vibrational Frequencies for HZnCH and Isotopic Derivatives

	HZnCH			HZn^{13}CH		DZnCD		
symmetry	ω	ω^a	ν	ω	ν	ω	ν	description
σ	3358	3393		3348		2478		C−H stretch
	2032	1972	1924	2032	1924	1449	1387	Zn−H stretch
	666	660	648	645	628	640	627	Zn−C stretch
π	488	452	469	487	469	356	345	cis bending
	206	162i		205		159		trans bending

[a] Hartree−Fock values from ref 2.

Under $C_{\infty v}$ constraint the electronic structure of zinc stannyne is rather similar to that of its parent; however, neither the triplet $^3\Sigma^-$ nor the singlet $^1\Delta$ are true minima on the potential energy surface, and both states distort with loss of linearity. The triplet $^3\Sigma^-$ leads to two equivalent $^3A''$ structures with HSnZn angles close to 120°, while in the Δ states there is a strong electronic coupling, mainly with the ground state of SnH, the $^2\Pi$ states, with a large stabilization of the $^1A'$ component, which is in fact the ground state of the complex. The nonclassical distortions of the $^3\Sigma^-$ and the $^1\Delta$ states in HZnSnH can be related to the higher gap between s and p tin levels or, according to the Trinquier and Malrieu[3] predictions, to the higher $^2\Pi-^4\Sigma^-$ split in SnH with respect to CH.

Acknowledgment. This work was supported by the DGICYT (Spain, Project No. PB92-0662) and by the European Commission (Contract No. ERBCT1-CT94-0064).

References and Notes

(1) Chang, S.-C.; Haige, R. H.; Kafafi, Z. H.; Margrave, J. L.; Billups, W. E. *J. Chem. Soc., Chem. Commun.* **1987**, 1682.

(2) Hamilton, T. P.; Schaefer, H. F. *J. Chem. Soc., Chem. Commun.* **1991**, 621.

(3) Trinquier, G.; Malrieu, J. P. *J. Am. Chem. Soc.* **1987**, *109*, 5303.

(4) For recent reviews, see: (a) Collman, J. P.; Hegedus, L. S.; Norton, J. R.; Finke, R. G. *Principles and Applications of Organotransition Metal Chemistry*; University Science Books: Mill Valley, CA, 1987. (b) Stephan, D. W. *Coord. Chem. Rev.* **1989**, *95*, 41. (c) Adams, R. D. *Chem. Rev.* **1989**, *89*, 1703. (d) Adams, R. D., Herrmann, W. A., Eds. The Chemistry of Heteronuclear Clusters and Multimetallic Catalists. *Polyhedron* **1988**, *7*, 2251. (e) Zanello, P. *Coord. Chem. Rev.* **1988**, *87*, 1. (f) *Organometallic Chemistry*; Stone, F. G. A.; Abel, E. W., Eds.; Royal Society of Chemistry: London, 1990; Vol. 18 and earlier volumes.

(5) Fischer, E. O.; Maasbol, A. *Angew. Chem., Int. Ed. Engl.* **1964**, *3*, 580. Fischer, E. O. *Adv. Organomet. Chem.* **1976**, *14*, 1.

(6) Schrock, R. R. *J. Am. Chem. Soc.* **1975**, *97*, 6578. Schrock, R. R. *Acc. Chem. Res.* **1979**, *12*, 98. Schrock, R. R. *Acc. Chem. Res.* **1990**, *23*, 158.

(7) For comprehensive reviews, see: (a) Dotz, K. H.; Fisher, H.; Hofmann, P.; Kreissl, F. R.; Schubert, U.; Weiss, K. *Transition Metal Carbene Complexes*; Verlag Chemie: Deerfield Beach, FL, 1984. (b) Cardin, D. J.; Cetinkaya, B.; Lappert, M. F. *Chem. Rev.* **1972**, *72*, 545.

(8) San Miguel, M. A.; Márquez, A.; Fernández Sanz, J. *J. Am. Chem. Soc.*, in press.

(9) Márquez, M.; Fernández Sanz, J. *J. Am. Chem. Soc.* **1992**, *114*, 10019.

(10) Stevens, W. J.; Basch, H.; Krauss, M. *J. Chem. Phys.* **1984**, *81*, 6026. Stevens, W. J.; Krauss, M.; Basch, H.; Jasien, P. G. *Can. J. Chem.* **1992**, *70*, 612.

(11) Dunning, T. H. In *Modern Theoretical Chemistry*; Schaefer, H. F., Ed.; Plenum Press: New York, 1977; Vol. 2. Huzinaga, S. *J. Chem. Phys.* **1965**, *42*, 1293.

(12) Complete active space SCF: Roos, B. O.; Taylor, P. M.; Siegbahn, P. E. M. *Chem. Phys.* **1980**, *48*, 157. Siegbahn, P. E. M.; Almlöf, J.; Heiberg, A.; Ross, B. O. *J. Chem. Phys.* **1981**, *74*, 2384. Roos, B. O. *Int. J. Quantum Chem.* **1980**, *S14*, 175.

(13) Frisch, M. J.; Trucks, G. W.; Head-Gordon, M.; Gill, P. M. W.; Wong, M. W.; Foresman, J. B.; Johnson, B. G.; Schlegel, H. B.; Robb, M. A.; Replogle, E. S.; Gomperts, R.; Andres, J. L.; Raghavachari, K.; Binkley, J. S.; Gonzalez, C.; Martin, R. L.; Fox, D. J.; Defrees, D. J.; Baker, J.; Stewart, J. J. P.; Pople, J. A. *Gaussin-92;* Gaussian, Inc.: Pittsburgh, PA, 1992.

(14) Dupuis, M.; Chin, S.; Márquez, A. CHEM-Station and HONDO: Modern Tools for Electronic Structure Studies Including Electron Correlation. In *Relativistic and Electron Correlation Effects in Molecules and Clusters*; Malli, G. L., Ed.; NATO ASI Series; Plenum Press: New York, 1994.

(15) Fernández Sanz, J.; Márquez, A.; Anguiano, J. *J. Phys. Chem.* **1992**, *96*, 6974. Márquez, A.; González, G. G.; Fernández Sanz, J. *Chem. Phys.* **1989**, *138*, 99.

(16) Villar, H. O.; Dupuis, M. *Chem. Phys. Lett.* **1987**, *142*, 59, and references cited therein.

(17) Herzberg, G.; Teller, E. *Z. Phys. Chem.* **1933**, *B21*, 410. Renner, R. *Z. Phys. Chem.* **1934**, *92*, 172. See, for instance: Herzberg, G. *Molecular Spectra Molecular Structure. III. Electronic Spectra and Electronic Structure of Polyatomic Molecules*; Van Nostrand-Reinhold: New York, 1966; p 26.

(18) Pople, J. A.; Longuet-Higgins, H. C. *Mol. Phys.* **1958**, *1*, 372.

(19) Huber, K. P.; Herzberg, G. *Constants of Diatomic Molecules*; Van Nostrand-Reinhold: New York, 1979.

(20) Hess, B. A., Jr.; Schaad, L. J.; Carsky, P.; Zahradnik, R. *Chem. Rev.* **1986**, *86*, 709.

(21) Haunge, R. H.; Margrave, J. L.; Kafafi, Z. H. In *Chemistry and Physics of Matrix-Isolated Species*; Andrews, L., Moskovits, M., Eds.; Elsevier: Amsterdam, 1989.

JP952199L